

$z_0$  increases from one or decreases from infinity. This strongly suggests that there is some maximum value of  $1/N(0)V$  as a function of  $z_0$ . This maximum represents the value of  $1/N(0)V$  for which  $X$  is the critical length  $X_c$ . For any value of  $1/N(0)V$  smaller than the maximum, there will be two corresponding values of  $z_0$ , representing the two possible superconducting solutions. For any value of  $1/N(0)V$  greater than the maximum, there corresponds no value of  $z_0$ , indicating that no superconducting solution exists.

Let us assume that Eq. (11.7) holds for all values of  $z_0$ . Then we clearly see that there is a maximum value

of  $1/N(0)V$  equal to  $(X/e\delta)^2$ , occurring at  $z_0=e^2$ . This gives

$$X_c = e\delta[N(0)V]^{-\frac{1}{2}}, \quad (11.8)$$

and

$$p/z_0 = 1/2N(0)V. \quad (11.9)$$

Equation (11.9) shows that when  $1/N(0)V \ll \frac{1}{2}$ , it is indeed true that  $p \ll z_0$  (so that Eq. (11.7) holds true) for all values of  $z_0$ . Figure 2 shows that  $X_c$  varies as  $[N(0)V]^{-\frac{1}{2}}$  and  $z \rightarrow z_0 \rightarrow e^2$  as  $1/N(0)V \rightarrow 0$ . However, over the range of interest of  $1/N(0)V$  (i.e., 2-5), Eq. (11.8) is not a good approximation to  $X_c$ .

## Band Structure of Aluminum

WALTER A. HARRISON

*General Electric Research Laboratory, Schenectady, New York*

(Received January 4, 1960)

Calculations of the band energies at symmetry points in aluminum by Heine are extended into the zone using the pseudopotential interpolation scheme in order to obtain constant-energy curves in the neighborhood of the Fermi surface. In conjunction with this calculation, the lines of contact between various bands are found in detail. The de Haas-van Alphen effect, cyclotron-resonance effect, anomalous skin effect, and low-temperature specific heat are discussed in terms of these constant-energy curves and the results compared with experiment. It appears from this comparison that the geometry of the Fermi surface is given quite well by the band calculations, but that there is a discrepancy of a factor of order two between the derived and measured effective masses. A "single orthogonalized-plane-wave approximation" is compared with the more exact treatment and found to be a good starting approximation, suitable for semiquantitative treatment of the electronic structure.

### I. INTRODUCTION

**F**OLLOWING the remarkable success of Gold<sup>1</sup> in understanding extensive de Haas-van Alphen data on lead in terms of a "nearly-free-electron approximation", the author<sup>2</sup> applied the same method to existing data on aluminum. Again, the data seemed to fit quite closely that to be expected on the basis of this very simple model. In view of the success of this model in understanding the de Haas-van Alphen effect, it is desirable to consider the band structure of one of these metals in detail in order to see to what extent the simple model describes the actual band structure.

In the following sections the orthogonalized-plane-wave (OPW) calculations for aluminum by Heine<sup>3</sup> are extended to obtain constant-energy curves in wave-number space. These are compared with a "single-OPW approximation," the latter being equivalent to the "nearly-free-electron approximation" in its application. Finally, the descriptions of the de Haas-van Alphen effect, cyclotron-resonance effect, anomalous skin

effect, and low-temperature specific heat derived from the two points of view are compared with each other and with experiment.

### II. ENERGY-BAND CALCULATIONS

Heine<sup>3</sup> has calculated the energies of the bands at several points of high symmetry in the band using the orthogonalized-plane-wave method. In order to consider the behavior of the electron gas in aluminum, we require knowledge of the energy bands at more general points in the zone, and in particular near the Fermi surface. Heine<sup>4</sup> has indicated that in the first two bands the energy is quite close to the free-electron value except near the zone faces. This suggests<sup>5</sup> that in most of the band the wave functions may be fairly well described by a single OPW. This further suggests that near a zone face only two are necessary; near a zone edge, three; and near a zone corner, four. Finally, consideration of the zones in aluminum indicates that the mixing of OPW's in the region of interest should be describable in terms of only two independent off-diagonal matrix elements of the Hamiltonian. Thus

<sup>1</sup> A. V. Gold, Phil. Trans. Roy. Soc. (London) **A251**, 85 (1958).

<sup>2</sup> W. A. Harrison, Phys. Rev. **116**, 555 (1959).

<sup>3</sup> V. Heine, Proc. Roy. Soc. (London) **A240**, 361 (1957). (Heine III).

<sup>4</sup> V. Heine, Proc. Roy. Soc. (London) **A240**, 340 (1957). (Heine I).

<sup>5</sup> M. H. Cohen and V. Heine, Suppl. Phil. Mag. **7**, 395 (1958).

we may hope to fit these two using Heine's results at symmetry points and obtain the energy at a general point by the solution of a secular equation of order four at most.

It would seem at first quite surprising that the lattice potential may be sufficiently weak that this limited number of plane waves is enough. However, Phillips and Kleinman<sup>6</sup> have indicated that the orthogonalization to the core states has the effect of introducing a pseudopotential which tends to cancel the lattice potential and to reduce the matrix elements between various OPW's. Cohen<sup>7</sup> has found that this cancellation is not fortuitous and that it may be expected in metals under fairly general circumstances. Thus our approach is essentially the pseudopotential interpolation scheme of Phillips<sup>6</sup> with the necessary parameters determined from Heine's band calculation. It will be possible to determine these parameters from his energy values at the single symmetry point  $W$  and from these determine the energies everywhere else in the band. Our values at other symmetry points may be compared with those of Heine as a check on the reliability of the scheme.

The pseudopotential approach is essentially the following. We assume the existence of a self-consistent potential,  $V(\mathbf{r})$ . The Hamiltonian,  $p^2/2m + V(\mathbf{r})$ , has a large number of one-electron solutions,  $\phi_i(\mathbf{r})$ , corresponding to core states. We take, as a starting approximation for the remaining states, plane waves orthogonalized to the  $\phi_i(\mathbf{r})$ ; thus the Hamiltonian operating on the core states yields only core states, and operating on the plane-wave states yields only plane-wave states. We may therefore consider the plane-wave or conduction-band states,  $\psi_{\mathbf{k}}$ , separately. Such plane-wave states having wave numbers differing by a reciprocal lattice vector will not be orthogonal to each other. The nonorthogonality in this case will be included only to the extent that it may be represented as a contribution to a pseudopotential, so nonorthogonality terms do not appear explicitly. The pseudopotential,  $V_p$ , is defined<sup>6</sup> as the potential which will give a good fit to the conduction-band energies. The effective Hamiltonian is given by

$$H = T + V_p(\mathbf{r}),$$

$$H = \begin{bmatrix} T[\mathbf{k}] & V_{200} & V_{111} & V_{111} \\ V_{200} & T[\mathbf{k} - (0,0,2)] & V_{111} & V_{111} \\ V_{111} & V_{111} & T[\mathbf{k} - (1,1,1)] & V_{200} \\ V_{111} & V_{111} & V_{200} & T[\mathbf{k} - (1,-1,1)] \end{bmatrix}, \quad (1)$$

where  $T[\mathbf{k}]$  is the energy of a single OPW of wave number  $\mathbf{k}$ , and  $V_{200}$  and  $V_{111}$  are the appropriate Fourier components of the pseudopotential. The basis

<sup>6</sup> J. C. Phillips, Phys. Rev. **112**, 685 (1958), and J. C. Phillips and L. Kleinman, Phys. Rev. **116**, 287 (1959).

<sup>7</sup> M. H. Cohen (private communication).

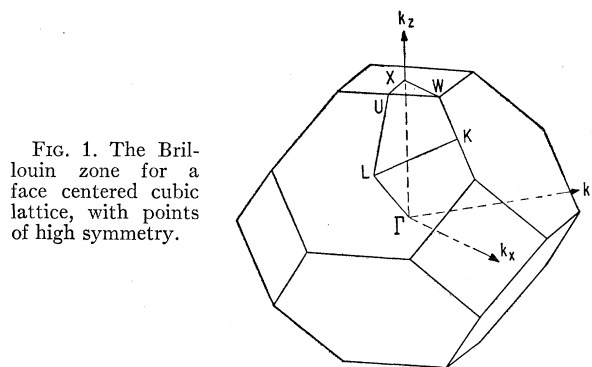


FIG. 1. The Brillouin zone for a face centered cubic lattice, with points of high symmetry.

where  $T$  is a kinetic-energy-like term and  $V_p(\mathbf{r})$  is to be treated as a simple, wave-number-independent potential. The pseudopotential may be expanded in Fourier components,

$$V_p = \sum_{\mathbf{K}} V_{\mathbf{K}} e^{i\mathbf{K} \cdot \mathbf{r}},$$

where the  $\mathbf{K}$  are reciprocal lattice vectors. The  $V_{\mathbf{K}}$ , then, are the matrix elements connecting plane waves differing in wave number by  $\mathbf{K}$ . If the pseudopotential is weak, as we expect, then the  $V_{\mathbf{K}}$  will be small, and the interaction of two plane-wave states, differing in wave number by  $\mathbf{K}$ , will be important only if the energies of those states are nearly the same. In free-electron language, states will mix only if a Bragg reflection is possible between them, allowing a slight nonconservation of energy. Thus only a few orthogonalized plane waves need be considered at one time, and a secular equation of low order is sufficient.

Consider first the bands in the region of  $W$  in the face-centered-cubic Brillouin zone, shown in Fig. 1. Taking as the unit of wave number the distance  $\Gamma X$ , which equals  $2\pi/a = 0.823$  atomic units for aluminum, the symmetry point  $W$  is located at  $(\frac{1}{2}, 0, 1)$ , as measured from  $\Gamma$ . An OPW of wave number  $\mathbf{k}$  in the region of  $W$  has matrix elements connecting it with OPW's of wave numbers  $\mathbf{k} - (0,0,2)$ ,  $\mathbf{k} - (1,1,1)$ , and  $\mathbf{k} - (1,-1,1)$ , these four waves having similar energies. Mixing with all other states is neglected and the Hamiltonian matrix is written

vectors are, of course, the individual OPW's.  $T[\mathbf{k}]$  may be taken to be spherically symmetric if neighboring core states do not overlap and, in particular, it is set equal to  $\alpha k^2$  with  $\alpha$  to be adjusted. This is somewhat crude, but will be justified by the suitable agreement with Heine at the various symmetry points. The

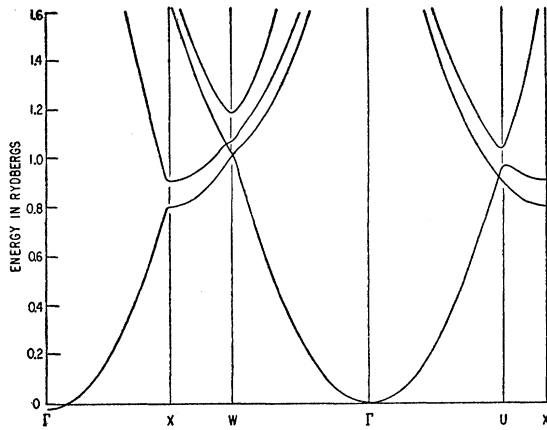


FIG. 2. Energy versus wave number along various symmetry lines, obtained using a four-OPW approximation and fitting Heine's values at  $W$ . The curves  $\Gamma X$  were obtained using only two OPW's, giving rise to the discrepancy at  $\Gamma$  on the left.

eigenvalues of (1) for  $\mathbf{k}$  at  $W$  are readily found and are given by

$$E = 1.25\alpha - V_{200}, \text{ and } 1.25\alpha + V_{200} \pm 2V_{111}, \quad (2)$$

where the first level given is degenerate. These may be equated to the values given by Heine,<sup>3</sup> 1.012 ry (degenerate), 1.063 ry, and 1.182 ry. This yields

$$\alpha = 0.8535 \text{ ry}, V_{200} = 0.0550 \text{ ry}, \text{ and } V_{111} = 0.0295 \text{ ry}. \quad (3)$$

The off-diagonal elements are small as expected.

Using the parameters given in (3), the eigenvalues of (1) have been found for  $\mathbf{k}$  running along various lines of symmetry. The results are displayed in Fig. 2. Such a calculation is not completely consistent since at each symmetry point, other than  $W$ , at least one other OPW has been neglected which would make a contribution equal to one which has been included. The addition of such plane waves, however, would not have an appreciable effect on the curves in the energy range of Fig. 2. The magnitudes of the errors involved may be seen from the discrepancy between the two energy values given at  $\Gamma$ . The curves  $\Gamma X$  were calculated using only two OPW's and shifted to fit the four OPW calculation at  $X$ , whereas all other curves involved the four orthogonalized plane waves.

TABLE I. Energy in rydbergs.

	Heine I	Heine III	4-OPW
$\Gamma_1$	0.000	0.000	0.000
$W_3$	1.036	1.012	1.012
$W_2'$	1.041	1.063	1.063
$W_1$	1.250	1.182	1.182
$X_4'$	0.867	0.806	0.799
$X_1$	0.925	0.929	0.905
$K_3 U_3$	0.950	0.925	0.905
$K_1 U_1$	0.948	0.966	0.937
$K_1 U_1$	1.078	1.298	1.033

Perhaps a more significant estimate of the error in our procedure may be obtained by comparing the values we obtain at symmetry points with those obtained by Heine. Table I gives the values obtained by Heine in a preliminary calculation (Heine I),<sup>4</sup> and in his self-consistent calculation (Heine III),<sup>3</sup> along with those obtained with four OPW's. The first four points have been adjusted to fit Heine III. The remaining five points are seen to agree within 0.03 rydbergs except for the third-band value at  $K$ . The value 1.298 given by Heine at this point appears anomalous not only with respect to the four-OPW calculation, but also with respect to that in Heine I, and it is reasonable to suppose that this value is in error. Agreement within 0.03 rydbergs for the remaining states is sufficient for our purposes.

It is of interest to compare these curves with those obtained by letting  $V_{200}$  and  $V_{111}$  become vanishingly

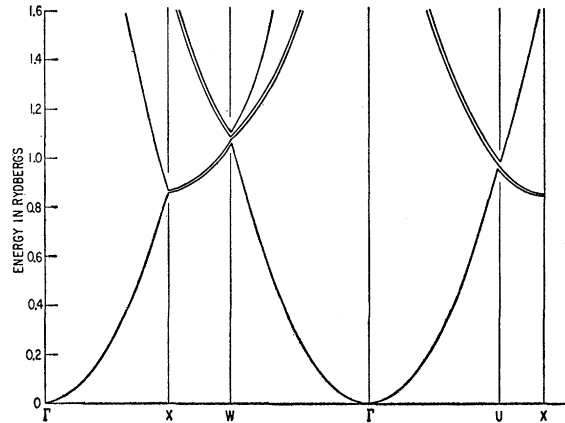


FIG. 3. Energy versus wave number along various symmetry lines, obtained using a single-OPW approximation; this is equivalent to the "nearly-free-electron approximation" and to the "empty-lattice" band structure described by F. Herman [Revs. Modern Phys. 30, 102 (1958)]. The vertical scale corresponds to an effective mass of 0.79. Close parallel lines represent degeneracies.

small; that is, by going to the one-OPW limit. In doing this we maintain the connectivity between different segments of the curves as determined by nonzero off-diagonal matrix elements. These curves are presented in Fig. 3. Such comparison would suggest that the one-OPW approximation was quite bad. However, the points displayed are those which lie on symmetry lines and are therefore just those for which we expect the single-OPW approximation to be worst. When we proceed to examine states near the Fermi surface, we will find the situation very much better.

### III. CONSTANT ENERGY CURVES

In studying the electronic properties of aluminum, we will be interested only in the states near the Fermi surface. Curves such as those in Fig. 2 give us only a few points at the Fermi energy and a great deal of information about regions which are not of interest.

Ideally one would like the intersections of the Fermi surface and neighboring constant-energy surfaces with planes in the Brillouin zone. These not only give the shape of the Fermi surface, but also give the Fermi velocity along a line on the Fermi surface and enable one to determine various electronic properties directly. Although such curves are very difficult to obtain in a full band calculation, they may readily be determined when only a few plane waves are involved. A convenient procedure is outlined in Appendix I. The shapes of the surfaces are somewhat complicated by lines of contact between neighboring bands; that is, by lines of accidental degeneracy. These may intersect the constant energy surfaces and give rise to conical cusps on the surfaces. A determination of the location of such lines of contact is given in Appendix II. It is not easy to determine the value of the Fermi energy exactly, but we may expect it to be fairly close to the single-OPW value of 1.084 ry, so surfaces with energy in this range have been determined.

The significance to be attached to these curves is

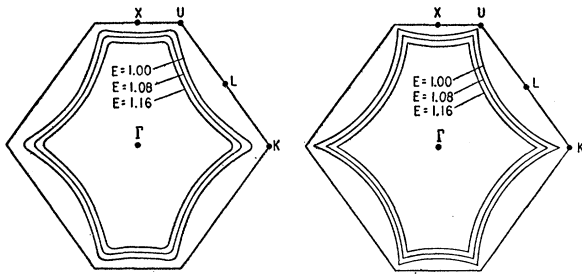


FIG. 4. Intersection of constant-energy surfaces in the second band with a (110) plane through  $\Gamma$ . The energies with respect to  $\Gamma$  for each curve are given in rydbergs. The curves to the left correspond to a four-OPW approximation; those on the right, to a single-OPW approximation.

questionable in view of uncertainties of the order of 0.03 rydbergs in our calculated energies. Thus the energies in one region of the Brillouin zone may be shifted appreciably with respect to those in another region. However, the errors are not significantly worse than those of the original band calculation on which they are based, and the main features of the curves are certainly not seriously in error. We will partially compensate for such errors by evaluating the Fermi energy experimentally with respect to these bands in Sec. IV, and keep the uncertainty in mind in interpreting the results.

Figures 4, 5, and 6 give the constant-energy curves for three cases of interest. In Figs. 5 and 6 various pieces of the constant-energy surfaces have been translated by reciprocal lattice vectors to obtain closed surfaces.<sup>8</sup> The curves obtained from a single-OPW approximation are given for comparison. The way in

<sup>8</sup> Such a procedure has been discussed in relation to the "nearly-free-electron approximation" by Gold (reference 1) and the author (reference 2).

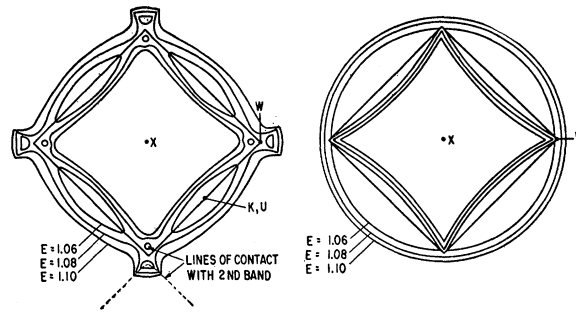


FIG. 5. Intersection of constant-energy surfaces in the third band with a (100) plane through  $X$ . The energies with respect to  $\Gamma$  for each curve are given in rydbergs. The curves to the left correspond to a four-OPW approximation; those on the right, to a single-OPW approximation.

which the constant energy surfaces extend out of these planes can be seen from Fig. 7 in which the Fermi surface in the single-OPW approximation is drawn in three dimensions.<sup>9</sup>

It is seen that the main effect of mixing in additional OPW's is to round off edges of the Fermi surface which are sharp in the single-OPW approximation. In the third band this brings about significant changes in the various cross-sectional areas, but the single-OPW approximation is still satisfactory for seeing qualitative features of the surfaces and for making semiquantitative estimates. This, then, must be the reason for the success of the "nearly-free-electron approximation" in explaining the observed de Haas-van Alphen oscillations; although single free-electron plane waves are quite poor approximations to the wave functions, single OPW's may be sufficiently close to give a good approximation to the energy.

In the following section we will use these curves to discuss the electronic properties of aluminum. We will compare the single-OPW approximation with the more

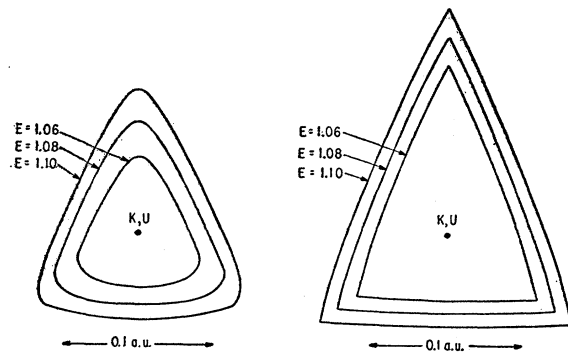


FIG. 6. Intersection of constant-energy surfaces in the third band with a (110) plane through  $K$ . The energies with respect to  $\Gamma$  for each curve are given in rydbergs. The curves to the left correspond to a three-OPW approximation, with energies corrected to correspond to a four-OPW approximation; those on the right, to a single-OPW approximation.

<sup>9</sup> This figure has been taken from reference 2. The general features of the entire Fermi surface are discussed in this reference.

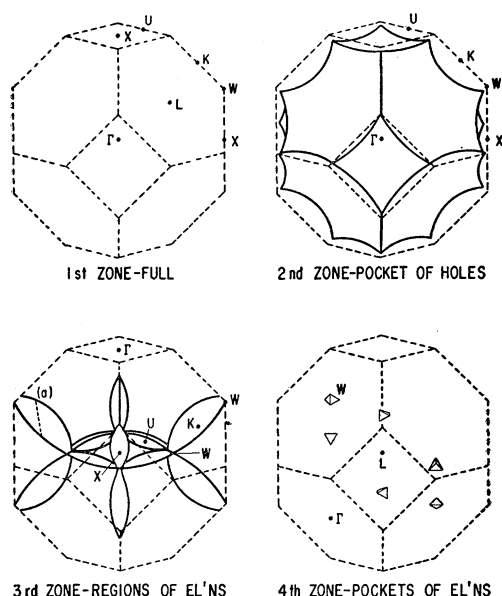


FIG. 7. The Fermi surface of aluminum according to the single-OPW, or to the nearly-free-electron, approximation. In this approximation six small pockets occur in the fourth band, but these disappear upon the addition of more OPW's. The first band is completely full.

exact calculation, and with experimental results where they exist.

#### IV. ELECTRONIC PROPERTIES

##### 1. The de Haas-van Alphen Effect

The de Haas-van Alphen Effect has been studied extensively in aluminum by Gunnensen.<sup>10</sup> The high-frequency oscillations are believed<sup>2</sup> to be associated with orbits around the "arms" in the third band. The maximum period corresponds to an area in wave-number space of 0.0075 atomic units and would be represented by a line on the constant-energy surface such as those shown in Fig. 6.

The areas of the three constant-energy curves shown in Fig. 6 are 0.0046 atomic unit for  $E=1.06$ ; 0.0090 atomic unit for  $E=1.08$ , and 0.0136 atomic unit for  $E=1.10$ . If we were to assume that the Fermi energy is equal to the single-OPW value of 1.084 rydbergs, we obtain an area of 0.010, to be compared with the experimental value of 0.0075. Actually, the introduction of the potential will lower the Fermi energy slightly; a Fermi energy of 1.075 rydbergs would give an area equal to 0.0075 atomic unit in agreement with experiment.

According to the curves of Fig. 5, an energy as low as 1.075 would pinch off the arms near the ends (in the manner indicated by the 1.06 rydberg curve of Fig. 5). If this, in fact, happens it would be necessary to attribute the low-frequency oscillations observed

by Gunnensen<sup>10</sup> to the small sections of surface around the lines of contact rather than with minimum cross sections of the arms near the ends as proposed earlier.<sup>2</sup> An energy of 1.078 would not pinch the arms off, on the other hand. Thus the calculation here is certainly not reliable enough to decide on this point; nor is the data complete enough to decide, and this question remains open.

The cross-sectional area on the basis of the *single-OPW* approximation is 0.015 atomic unit, in only semiquantitative agreement with the experimental value of 0.0075. As has been seen from the investigations of lead<sup>1</sup> and aluminum,<sup>2</sup> however, this is sometimes sufficient to allow interpretation of the experimental results.

The temperature dependence of the de Haas-van Alphen oscillation amplitudes gives information about the cyclotron masses of the carriers in question. However, since the masses found by Gunnensen are consistent with those found in the more recent direct observation of cyclotron resonance,<sup>11,12</sup> we will discuss the question of masses in connection with those experiments.

##### 2. Cyclotron Resonance

In the presence of a magnetic field an electron orbit in wave-number space is given by the intersection of a plane perpendicular to the magnetic field and a constant energy surface. Thus the curves of Figs. 4 and 6 correspond to electron orbits for a magnetic field lying in a (110) direction; those of Fig. 5 correspond to a field in a (100) direction. The cyclotron mass is determined from the change in the area of these orbits with energy by

$$\frac{m^*}{m} = \frac{1}{\pi} \frac{dA}{dE},$$

where  $A$  is in atomic units and  $E$  is in rydbergs. Thus the masses are directly obtainable from figures such as those shown. The masses obtained from Figs. 4 and 6 are 0.60 and 0.072, respectively, and do not depend sensitively on energy.

Langenberg and Moore<sup>11</sup> and Fawcett<sup>12</sup> have observed cyclotron resonance in aluminum. Fawcett finds a mass of 0.11 for a field parallel to the (110) axis. This and the other masses observed at this and at other orientations are consistent within about 15% with the picture of cylindrical pieces of Fermi surface lying along each (110) direction, with a mass of 0.11 associated with the field parallel to the cylinder axis.<sup>13</sup> In addition, this mass is of the same order as that

<sup>11</sup> D. N. Langenberg and T. W. Moore, Phys. Rev. Letters 3, 137 (1959).

<sup>12</sup> E. Fawcett, Phys. Rev. Letters 3, 139 (1959).

<sup>13</sup> In making this comparison we note that the mass goes as  $1/\cos\theta$  for a cylindrical surface,  $\theta$  being the angle between the field and the cylinder axis; see J. M. Ziman, Phil. Mag. 3, 1117 (1958).

<sup>10</sup> E. M. Gunnensen, Phil. Trans. Roy. Soc. (London) A249, 299 (1957).

found by Gunnarsen for the oscillations we attribute to the third-band arms. Thus we associate the mass 0.11 with the section shown in Fig. 6 and compare it to our calculated mass of 0.072. The agreement, which is not as good as one might hope, will be discussed after consideration of further cyclotron-resonance measurements.

Langenberg and Moore observed a resonance which presumably corresponds to the carriers observed by Fawcett. They found a mass of 0.18 with a field in the (111) direction, to be compared to 0.13 to be expected on the basis of the model mentioned above with Fawcett's values. In addition, they observed a high-mass resonance corresponding to a mass of 1.5 which was quite isotropic (within 10%). This is presumably to be associated with the second band and with orbits of the type illustrated in Fig. 4, for which we obtained a mass of 0.60.

Again our calculated mass is significantly below that observed. It is conceivable that the observed mass is associated with other orbits than those considered, but this seems unlikely. Although resonances associated with other portions of the surface are possible, the extremal orbits considered here should be the most pronounced.<sup>14</sup>

A significant error in our formula for the single-OPW energy,  $T = \alpha k^2$ , could give rise to large errors in our calculations of the mass without disturbing the agreement with the de Haas-van Alphen data; a value of  $\alpha$  about half of what we used would bring the masses up to the vicinity of those observed. Furthermore, if  $\alpha$  were a function of  $k$  and were lowered for high  $k$  and raised for low  $k$ , this agreement could be achieved without changing the total band width. Such changes, however, would involve rather major inconsistencies with the band calculation. The difference between the Bohm-Pines<sup>15</sup> expression for  $T$  and the parabola used here is much too small to be of interest in this comparison.

At this point we must conclude that the band calculation is only in semiquantitative agreement with experiment and that we do not know the source of the discrepancy.

The masses obtained with the single-OPW approximation, using  $T = 0.835k^2$  in our units, are within a few percent of those resulting from the four-OPW approximation; this corresponds to an effective mass at the bottom of the band of 0.79. If we were to use an effective mass of unity, rather than 0.79, then  $T = 0.677k^2$  and the agreement with experiment is slightly improved. In any case, the single-OPW approximation should be regarded as semiquantitative and sufficiently crude with respect to mass determinations that the mass-one parabola is suitable.

<sup>14</sup> J. C. Phillips, Phys. Rev. Letters 3, 327 (1959). See also discussion in the paper following the present one.

<sup>15</sup> The Bohm-Pines form [D. Pines, *Solid State Physics* edited by F. Seitz and D. Turnbull (Academic Press, New York, 1955), Vol. 1, p. 368] was used by Heine (reference 4).

### 3. Anomalous Skin Effect

An anomalous-skin-effect measurement on a polycrystalline sample gives a measure of the total area of the Fermi surface. The total area for the single-OPW approximation is just equal to the free-electron area; the alteration of the connectivity of various pieces of the surface does not influence the result. The four-OPW approximation would give a slightly reduced area, since by rounding off the edges of the surface one reduces the area. Heine has indicated that the existing data imply an area about equal to the free-electron area, but this result is quite uncertain.<sup>16</sup> The measured surface resistances quoted by Faber and Pippard<sup>17</sup> vary as much as 10% from the average, and the Fermi surface area varies as the third power of resistance.

The single-OPW approximation would give an isotropic anomalous skin effect, but the inclusion of more plane waves would yield anisotropies. There do not exist at present published data on single crystals of aluminum, and the theoretical picture will be postponed to the adjoining paper on the single-OPW approximation.

### 4. Low-Temperature Specific Heat

The electronic specific heat, like cyclotron resonance, depends upon  $dE/dk$  at the Fermi surface as well as upon the geometry of the surface. Thus we may expect discrepancies of the sort which we found with cyclotron resonance. The electronic specific heat is proportional to  $dV/dE$ , where  $V$  is the Fermi volume in wave-number space associated with a surface of constant energy  $E$ . The single-OPW approximation gives  $dV/dE$  equal to the free-electron value if a free-electron parabola is used. If one takes the energy to be given by  $0.8535k^2$  for a single-OPW approximation as suggested by the band calculation, one obtains a  $dV/dE$  which is smaller than the free electron value by 20%. The experimental specific heat as measured by Howling, Mendoza, and Zimmerman<sup>18</sup> is, as Heine pointed out, 1.6 times the free-electron value. Thus, as in the cyclotron-resonance case, we are in error by a factor of order two.

Heine<sup>4</sup> and the author<sup>2</sup> have previously attributed the discrepancy in the specific heat to regions of low  $dE/dk$  where the Fermi surface intersects symmetry planes. The four-OPW calculations would indicate that this is not as large an effect as was expected. The differential volume associated with specific heat is simply an integral over the differential areas associated with the cyclotron mass, and the cyclotron masses were not altered appreciably in going from single- to

<sup>16</sup> The author is indebted to E. Fawcett for making this point to him.

<sup>17</sup> T. E. Faber and A. B. Pippard, Proc. Roy. Soc. (London) A231, 336 (1955).

<sup>18</sup> D. H. Howling, E. Mendoza, and J. E. Zimmerman, Proc. Roy. Soc. (London) A229, 86 (1955).

four-OPW's. Application of Heine's estimating procedure to the cyclotron mass yields a correction of over 15% to the cyclotron mass of Fig. 4 and about 50% to that of Fig. 6, whereas the more accurate 4-OPW calculation gives negligible corrections.

Thus we may say that the specific-heat data are consistent with the cyclotron-resonance data and the qualitative picture given here, but there remains an apparent discrepancy of a factor of two between the masses from the band calculation and those observed.

## V. CONCLUSIONS

We have found that for aluminum, at least, the energy values at symmetry points from a band calculation may be fairly reliably extended to the entire band using only a few orthogonalized plane waves. In particular, we find that it is possible to construct constant-energy curves in the region of the Fermi surface with very little labor. Such curves give not only the shape of the Fermi surface, but also the cyclotron masses for particular orbits. Proceeding in this way from the band calculations of Heine, we have considered the electronic properties of aluminum and find that the shape of the surface agrees as close as we can tell with experiments which see only the geometry of the surface (de Haas-van Alphen effect and anomalous skin effect). On the other hand, we find that we underestimate by a factor of about two the masses which determine the cyclotron-resonance frequency and the electronic specific heat. The source of the errors in the mass is not understood.<sup>19</sup>

In addition, we have considered the limiting case as the lattice potential becomes small; that is, the single-OPW approximation. In its application, this is equivalent to the nearly-free-electron approximation used by Gold and by the author in studying the de Haas-van Alphen effect. The single-OPW approximation is found to be in semiquantitative agreement with experiment with respect to both the geometry of the Fermi surface and the relevant masses. The main effect of the lattice potential is the change in the connectivity of pieces of the Fermi surface; this aspect is included in the single-OPW approximation. A finite lattice potential also rounds off the edges of the constant-energy surfaces which are sharp in the single-OPW approximation and may eliminate small pockets of electrons which may appear in the single-OPW approximation. The lattice potential, in the case of

aluminum, does not alter the cyclotron and specific heat masses to the extent that was previously expected.

In view of the success of the single-OPW approximation as a semiquantitative theory for interpretation of experimental results and its validity as a first approximation to more exact band calculations, its application to a wide variety of metals has been undertaken. This work appears in the adjoining paper.

## APPENDIX I. DETERMINATION OF CONSTANT ENERGY SURFACES

From curves such as those of Fig. 2 we obtain a few points on any given constant energy surface. It is convenient to calculate other points on the surface directly. To illustrate this procedure, we consider the region near  $K$  or  $U$  which is shown in Fig. 6.

An OPW at a point  $K$  or  $U$  differs by a reciprocal lattice vector from two other OPW's having the same energy. Therefore, in this region it is appropriate to consider a three-by-three Hamiltonian matrix. The wave numbers of the three OPW's of interest may be taken as  $(\frac{1}{4}, \frac{1}{4}, 1)$ ,  $(\frac{1}{4}, \frac{1}{4}, -1)$ , and  $(-\frac{3}{4}, -\frac{3}{4}, 0)$  in our units. (The distance  $\Gamma-X$  is one in these units.) We wish to consider states lying near these in the  $x=y$  plane; thus we consider wave numbers differing from these by  $\kappa = \kappa[(\cos\theta)/\sqrt{2}, (\cos\theta)/\sqrt{2}, \sin\theta]$ .

In analogy with Sec. II, we write the Hamiltonian

$$H = \begin{pmatrix} T_0 & V_{200} & V_{111} \\ V_{200} & T_1 & V_{111} \\ V_{111} & V_{111} & T_2 \end{pmatrix}, \quad (A1)$$

where

$$\begin{aligned} T_0 &= \alpha k_0^2 + \alpha \kappa^2 + 2\alpha \kappa[(\sqrt{2}/4) \cos\theta + \sin\theta], \\ T_1 &= \alpha k_0^2 + \alpha \kappa^2 + 2\alpha \kappa[(\sqrt{2}/4) \cos\theta - \sin\theta], \\ T_2 &= \alpha k_0^2 + \alpha \kappa^2 + 2\alpha \kappa[-(3\sqrt{2}/4) \cos\theta]. \end{aligned} \quad (A2)$$

$\alpha$ ,  $V_{111}$ , and  $V_{200}$  have been evaluated from Heine's results. We wish to specify an energy eigenvalue and determine the vectors  $\kappa$  which satisfy the secular equation derived from (A1).

For a given energy  $E$ , the set  $\kappa$  as determined from the three-by-three Hamiltonian of (A1) will differ slightly from the set which would be obtained from the four-by-four Hamiltonian of Eq. (1). This, however, will not significantly modify the shape of the constant-energy surfaces, and the slight change in area may be corrected for by changing the energy value to be used in the solution. For example, for  $\cos\theta = -1$ , the value of  $\kappa$  obtained from the four-by-four Hamiltonian for an energy 1.080 is 0.059. If we evaluate the energy from (A1) for  $\kappa = 0.059$  and  $\cos\theta = -1$ , we obtain 1.087. Thus we evaluate the set  $\kappa$  from the secular equation derived from Eq. (A1) for an energy 1.087 and this will be quite close to the constant energy surface derived from Eq. (1) for an energy 1.08.

In determining  $\kappa$ , it is not convenient to specify  $\theta$  and evaluate  $\kappa$  since this involves the solution of a sixth-order equation. If, on the other hand, we specify

<sup>19</sup> Note added in proof.—The occurrence of the mass 0.79 for the kinetic energy term arises from Heine's use of a Bohm-Pines (see footnote reference 15) correction for exchange and correlation, which probably gives the wrong sign for the effect. If we drop this correction before fitting, we obtain a mass of one. The effective mass at the Fermi surface may then be recorrected for exchange and correlation [J. F. Fletcher and D. C. Larson, Phys. Rev. **111**, 455 (1958)] raising the effective mass further. This appears not to remove all of the discrepancy. The remaining part may be due to the electron-phonon interaction [see, for example J. J. Quinn, Bull. Am. Phys. Soc. Ser. II, **5**, 199 (1960)].

$\kappa$ , we obtain a third-order equation in  $\cos\theta$ ; the three values of  $\cos\theta$  obtained correspond to three points on the constant energy surface.

The secular equation may be written

$$\begin{vmatrix} T_0 - E & V_{200} & V_{111} \\ V_{200} & T_1 - E & V_{111} \\ V_{111} & V_{111} & T_2 - E \end{vmatrix} = y^3 + (\eta/3)y + [- (2\alpha\kappa)^2 + 2V_{111}^2/3 - V_{200}^2 + \eta^2/3]y + \eta^3 - (2\alpha\kappa)^2\eta - 2V_{200}V_{111}^2 - \eta(2V_{111}^2 + V_{200}^2) = 0,$$

where

$$y = (3\alpha\kappa\sqrt{2}/2) \cos\theta, \quad \eta = E - \alpha k_0^2 - \alpha\kappa^2.$$

This can be evaluated by standard techniques for several values of  $\kappa$  to obtain the curves of Fig. 6.

#### APPENDIX II

Lines of contact are known<sup>20</sup> to lie near  $W$ , hence the four-by-four Hamiltonian must be used in determining the location of these. Consider the Hamiltonian of Eq. (1) with  $\mathbf{k} = (\frac{1}{2} + \kappa_x, \kappa_y, 1 + \kappa_z)$ . The four OPW's with their wave numbers are

$$\begin{aligned} \psi_1, & \quad (\tfrac{1}{2} + \kappa_x, \kappa_y, 1 + \kappa_z); \\ \psi_2, & \quad (\tfrac{1}{2} + \kappa_x, \kappa_y, -1 + \kappa_z); \\ \psi_3, & \quad (-\tfrac{1}{2} + \kappa_x, -1 + \kappa_y, \kappa_z); \\ \psi_4, & \quad (-\tfrac{1}{2} + \kappa_x, 1 + \kappa_y, \kappa_z). \end{aligned}$$

$$\alpha \begin{vmatrix} E_2' - E_1' + \kappa_x & -\sqrt{2}\kappa_y & \sqrt{2}\kappa_y \\ -\sqrt{2}\kappa_y & E_3' - E_1' & \kappa_x \\ \sqrt{2}\kappa_y & \kappa_x & E_4' - E_1' \end{vmatrix} = \alpha \begin{vmatrix} -2\kappa_x & -\sqrt{2}\kappa_y \\ -\sqrt{2}\kappa_y & -\kappa_x + 2(V_{200} - V_{111})/\alpha \end{vmatrix} = 0.$$

This yields the equation for the line of contact,

$$\kappa_y^2 = \kappa_x^2 - \frac{V_{200}^2 - V_{111}^2}{\alpha V_{200}} \kappa_x, \quad \kappa_z = 0. \quad (\text{A5})$$

The corresponding lines in the  $\kappa_y = 0$  plane lie at

$$\kappa_z^2 = \kappa_x^2 + \frac{V_{200}^2 - V_{111}^2}{\alpha V_{200}} \kappa_x, \quad \kappa_y = 0. \quad (\text{A6})$$

The energies at the line of contact may readily be evaluated for the  $\kappa_z = 0$  case from (A4);

$$E(\kappa) = \alpha(9/8 + \kappa_x + \kappa^2) - V_{200}, \quad \kappa_z = 0. \quad (\text{A7})$$

<sup>20</sup> C. Herring, Phys. Rev. 52, 365 (1937).

For  $\kappa = 0$ , the eigenvectors and eigenvalues are readily seen to be

$$\begin{aligned} \phi_1 &= (\psi_1 - \psi_2)/\sqrt{2}, & E_1(0) &= 9\alpha/8 - V_{200}; \\ \phi_2 &= (\psi_3 - \psi_4)/\sqrt{2}, & E_2(0) &= 9\alpha/8 - V_{200}; \\ \phi_3 &= (\psi_1 + \psi_2 - \psi_3 - \psi_4)/2, & E_3(0) &= 9\alpha/8 + V_{200} - 2V_{111}; \\ \phi_4 &= (\psi_1 + \psi_2 + \psi_3 + \psi_4)/2, & E_4(0) &= 9\alpha/8 + V_{200} + 2V_{111}. \end{aligned}$$

It is convenient to use these  $\phi$ 's to define a unitary transformation for general  $\kappa$ . Then the Hamiltonian takes the form

$$H = \alpha \begin{pmatrix} E_1' + \kappa_x & 0 & \sqrt{2}\kappa_x & \sqrt{2}\kappa_x \\ 0 & E_2' - \kappa_x & -\sqrt{2}\kappa_y & \sqrt{2}\kappa_y \\ \sqrt{2}\kappa_x & -\sqrt{2}\kappa_y & E_3' & \kappa_x \\ \sqrt{2}\kappa_x & \sqrt{2}\kappa_y & \kappa_x & E_4' \end{pmatrix}, \quad (\text{A3})$$

where  $E_i' = E_i(0)/\alpha + \kappa^2$ . Note the limiting form as  $\kappa$  goes to zero. Lines of contact can occur in either the plane defined by  $\kappa_z = 0$  or by  $\kappa_y = 0$ , since in these cases  $\phi_1$  or  $\phi_2$  become uncoupled to the others, and the bands may cross. We consider the case  $\kappa_z = 0$ ; the other line may be found by symmetry.

In the  $\kappa_z = 0$  plane,

$$E_1'(\kappa) = 9/8 + \kappa_x + \kappa^2 - V_{200}/\alpha. \quad (\text{A4})$$

A line of contact will occur when this is a solution of the secular equation for  $\phi_2, \phi_3$ , and  $\phi_4$ ; i.e., when

$$\begin{vmatrix} -\sqrt{2}\kappa_y & \sqrt{2}\kappa_y \\ -\kappa_x + 2(V_{200} - V_{111})/\alpha & \kappa_x \\ \sqrt{2}\kappa_y & -\kappa_x + 2(V_{200} + V_{111})/\alpha \end{vmatrix} = 0.$$

For the  $\kappa_y = 0$  case, it is

$$E(\kappa) = \alpha(9/8 - \kappa_x + \kappa^2) - V_{200}, \quad \kappa_y = 0. \quad (\text{A8})$$

The Eqs. (A5) through (A8) define four lines of contact; the values of  $V_{111}$  and  $V_{200}$  determine which bands contact along each. For aluminum, the line of contact between the second and third bands is shown in Fig. 5.

Clearly the above derivation is valid for contacts between the first four bands in any face-centered-cubic metal for which the four-OPW approximation is suitable. The unit of wave number is the distance  $\Gamma X$ ; the magnitudes of  $\alpha$ ,  $V_{111}$ , and  $V_{200}$  are chosen for the metal in question. The procedure is also readily generalized to other crystal structures.